

Проведено дослідження впливу прямої полярності на вихідні параметри сонячних елементів (СЕ) ІТО/CdS/CdTe/Cu/Au. Експериментально зафіксовано вплив електричного поля прямої полярності на вихідні параметри і світлові діодні характеристики СЕ ІТО/CdS/CdTe/Cu/Au, у яких відбулася деградація ККД. При витримці затемненого СЕ не менше 120 хвилин в електричному полі, наведеному зовнішньою постійною напругою величиною (0,5–0,9) В, спостерігається зростання ККД. Полярність електричного поля повинна відповідати прямому зміщенню $n-p$ гетеропереходу. Зростання ККД спостерігається лише у тому випадку, якщо при деградації приладової структури не встигли сформуватися дефекти, які за вказаний час витримки призводять до самовідновлюючих електричних мікропробів, що чередуються.

Встановлено, що зростання ККД відбувається за рахунок збільшення густини фотоструму, зменшення послідовного та збільшення шунтувального опорів СЕ. Покращення діодних характеристик відбувається завдяки кільком фізичним процесам. При подачі на СЕ напруги прямого зміщення, всередині діодної структури СЕ створюється електричне поле, яке підсилює вбудоване електричне поле тильного $p-p^+$ гетероперехода і пригнічує вбудоване електричне поле фронтального n^+-p гетероперехода. Це відбувається внаслідок того, що діоди включені на зустріч один одному. Величина напруги прямого зміщення не повинна перевищувати висоту потенційного бар'єру гетеропереходу. У цьому випадку на тильному $p-p^+$ гетеропереході та у прилеглих до нього з обох сторін областях будуть інтенсифіковані процеси пов'язані з транспортом атомів міді. Крім того, спостерігається перебудова комплексів точкових дефектів, що містять мідь, та фазові перетворення $Cu_{1-x}Te$ в $Cu_{2-x}Te$.

Також під впливом поля, індукованого прямозмичуючою напругою, частки Cu_{Cd} з області збіднення шару CdS почнуть рухатись у абсорбер. Це повинно знизити опір частини шару CdS і привести до зменшення ширини області збіднення з боку абсорбера, тим самим, забезпечити зростання спектральної чутливості СЕ в короткохвильовій і середньохвильовій областях сонячного спектру. Електродифузія додаткової кількості Cu_{Cd} в абсорбер повинна посилювати вищеописаний і пов'язаний з цим ефект підвищення спектральної чутливості, а значить і J_f приладів. На основі проведених досліджень був розроблений алгоритм відновлення ефективності СЕ ІТО/CdS/CdTe/Cu/Au і відбраковування деградованих приладових структур в складі працюючого модуля що працює

Ключові слова: телурид кадмію, деградація сонячного елементу, спосіб відновлення, вихідні параметри, світлові діодні характеристики

DEVELOPMENT OF A TECHNIQUE FOR RESTORING THE EFFICIENCY OF FILM ITO/CdS/CdTe/Cu/Au SCs AFTER DEGRADATION

N. Deyneko
PhD*

E-mail: natalyadeyneko@gmail.com

P. Kovalev

PhD, Associate Professor

Department of Fire and Rescue Training**

E-mail: kovalev10121963@ukr.net

O. Semkiv

Doctor of Technical Sciences, Vice Rector***

E-mail: semkiv@nuczu.edu.ua

I. Khmyrov

PhD

Department of Supervision and Prevention**

E-mail: khmyrov7771@gmail.com

R. Shevchenko

PhD, Senior Researcher*

E-mail: shevchenko605@i.ua

*Scientific Department of Problems of Civil Protection and Technogenic and Ecological Safety of the Scientific and Research Center**
**National University of Civil Defence of Ukraine
Chernyshevskaya str., 94, Kharkiv, Ukraine, 61023

1. Introduction

It is known that effectiveness of the CdTe-based solar cells (SC) reduces during operation. The authors of paper [1] suggested two mechanisms in the degradation of such solar cells. The first is predetermined by the generation of defects in the area of semiconductor contact, caused by excessive charge carriers and defects of semiconductor layers. The second relates to an increase in the potential barrier at the rear ohmic contact. According to studies [2, 3], for the case of forming a tunnel rear contact, the degradation of SC is predetermined by the diffusion and interphase interactions between a nano-sized copper layer and a base layer [4]. Thus,

degradation of SC renders relevance to the search for structural-technological solutions aimed at improving the degradation stability of the specified instrumental structures.

2. Literature review and problem statement

Despite the global development of solar power engineering, the effect of SC degradation under the action of light is typical for any photoconverter. The processes that define the mechanisms of SC degradation and, accordingly, the efficiency recovery techniques, have not been investigated enough. Among existing studies, the greatest attention was paid

to the-second generation SC [5, 6]. For example, paper [7] demonstrated a technique for recovering the second-generation SC using the light whose intensity is less than the intensity of the initial light source. The authors of works [8–10] investigated the specificity of CdTe-based SC degradation. Currently there are several hypotheses that offer different mechanisms of CdTe-based SC degradation. One of the first attempts to explain the mechanisms of degradation implied the consideration of processes of defects generation under the action of light. However, this theory could not explain the existence of samples resistant to degradation. The most popular now is the theories of electromigration, mainly copper, from metal contacts to the interface CdTe–CdS. The processes to form shunting defects have also been considered. Paper [11] shows that it is possible to form a network of shunting defects in the form of dendrites, and study [12] emphasizes a precursor mechanism. However, in most of these works, the authors note that the probability of the implementation of a given degradational mechanism becomes higher in proportion to a decrease in the thickness of a solar battery layers. However, the existence of exceptionally stable samples was confirmed that are not subject to aging, in addition, certain samples even showed an increase in efficiency over time. Papers [13, 14] considered one of the conditions for obtaining stable solar cells based on CdS/CdTe. It was stated that the necessary condition for creating such SC is to thermally treat CdTe in the atmosphere containing Cl₂. Typically, this treatment is conducted by depositing a thin film of CdCl₂ atop CdTe by heating in open air at a fixed temperature. However, this stage is impractical under large-scale production. The authors of work [15] replaced this treatment by using a gas (HCF₂Cl), which is stable, inert, and non-toxic at room temperature, and eliminates the stage of CdCl₂ evaporation, as well as the procedure for subsequent chemical etching.

Given the degradation processes of CdTe-based SC during operation, it is necessary to undertake a research aimed at the development of a recovery technique for such instrumental structures.

3. The aim and objectives of the study

The aim of this work is to develop a technique for restoring the efficiency of the film ITO/CdS/CdTe/Cu/Au SC after degradation.

To accomplish the aim, the following tasks have been set:

- to explore changes in the output parameters and light diode characteristics after the accelerated degradation of ITO/CdS/CdTe/Cu/Au SC;

- to explore changes in the output parameters and diode characteristics of ITO/CdS/CdTe/Cu/Au SC with different types of n-p heterojunctions after exposure to direct polarity voltage;

- to define the conditions for the recovery of efficiency of the film ITO/CdS/CdTe/Cu/Au SC after degradation.

4. Samples and methods to study the output parameters of ITO/CdS/CdTe/Cu/Au SC

The examined instrumental structures of ITO/CdS/CdTe/Cu/Au were obtained by the method of thermal vacuum evaporation. The equipment and conditions for obtaining the examined samples are described in detail in [3]. We applied

the ITO films (a mixed indium-tin oxide) using the method of non-reactive magnetron spraying at direct current at the laboratory setup VUP 5 applying the original material-saving magnetron. The length of a charge gap that represents the distance between the magnetron and the substrate was 70 mm. The power used by the magnetron was 0.2 W/cm². Temperature of the substrate (T_s) was 300 °C. Initial pressure in the vacuum chamber was 3×10^{-5} mm Hg, working pressure of the argon-air mixture during spraying was $(2.1\text{--}2.6) \times 10^{-2}$ mm Hg. In order to press the ITO mixtures that contain indium oxide (95 % by weight) and tin oxide (5 % by weight), we fabricated a specialized pressing machine (Fig. 1).

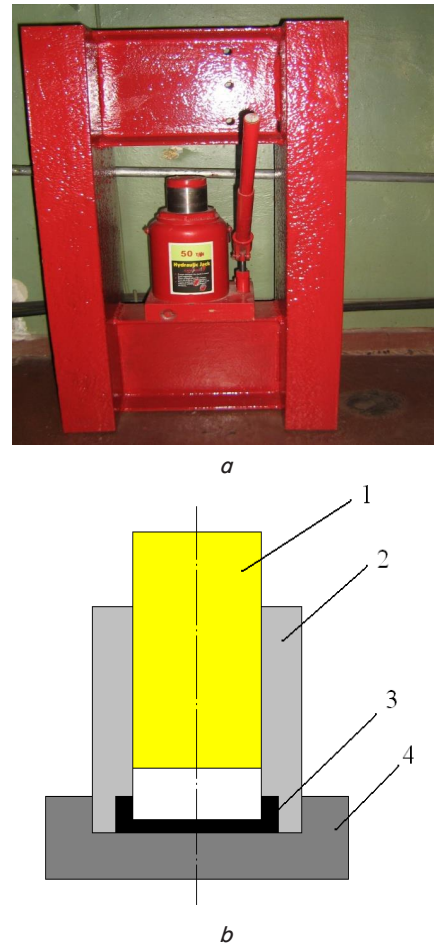


Fig. 1. Equipment for pressing the ITO mixtures: *a* – mechanical press; *b* – pressing matrix (1 – piston, 2 – cylinder, 3 – cylinder, 4 – stand)

It should be noted that magnetron spraying is one of the most promising methods for obtaining all transparent electrodes [16, 17]. This is predetermined by a high degree of precision when transferring the composition of a mixture onto the substrate, by reproducibility and control over the process of magnetron spraying [18, 19].

A matrix of the obtained solar cells is shown in Fig. 2. The initial values for efficiency coefficient of obtained SC were 9.4–10.4 %. Next, all SCs were placed in a non-transparent plastic sealed box with air medium typical of non-industrial premises. After 48 months, the box, which was kept over this time at a temperature of 15–25 xC, was unsealed to carry out a comprehensive research into the parameters of SC that were stored inside it. Among SCs on the matrix, which were exposed to the accelerated

degradation, part of SC was shunted. Among those suitable for recovery, we selected 7 SC samples to investigate the influence of a direct polarity voltage. Smooth (S) p–n junctions: two samples (No. 2, No. 6); unidentified (U) p–n junctions: three sample (No. 8, No. 12, No. 16); sharp (Sh) p–n junctions: two samples (No. 19, No. 20).

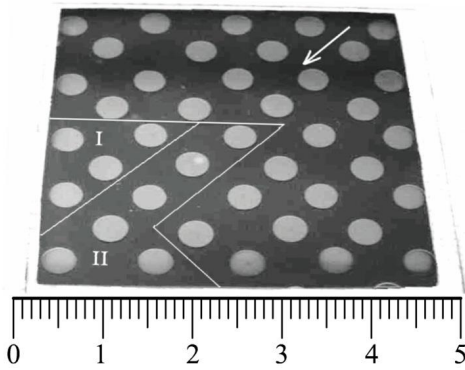


Fig. 2. Matrix of examined SC (the arrow shows a direction of the copper film thickness gradient, associated with the location of the source of copper during thermo vacuum deposition of the rear electrode); I – plot that belongs to SC with sharp n-p heterojunctions; II – plot that belongs to SC with smooth n-p heterojunctions

Selected samples were exposed to the action of a bias voltage of direct polarity $V_d^{\max} = 675 \pm 5$ mV at maximum duration $\tau_{\text{ex}} = 2$ hours under a shaded mode at room temperature, and then we acquired the current-voltage characteristic of light. We studied the light current-voltage characteristic for experimental samples under the following conditions: illumination – $1,000 \text{ W/m}^2$, solar spectrum – AM1,5, ambient temperature – $25 \text{ }^\circ\text{C}$. The equipment and methods to study the output parameters and the light diode characteristics for experimental samples are described in detail in paper [20]. The specified magnitude V_d^{\max} is chosen based on condition $V^{\max} < V_d \approx V_{oc}^{\min}$, where V^{\max} is the voltage that corresponds to the point of maximum power at the light current-voltage characteristic, and V_{oc}^{\min} is the smallest voltage of idling over the entire totality of values V_{oc} for the examined SC.

Development of the recovery method implies determining the dependence of SC efficiency on the effect of a bias voltage of direct polarity on it. It is known that efficiency of any SC is calculated from formula [21]:

$$\eta = (P_{nm} / P_r) \cdot 100\% = [P_{nm} / (P_r * S_s)] \cdot 100\%, \quad (1)$$

where P_r^* is the specific absorption rate at the SC photo-receiving surface; S_s is the area of SC photo-receiving surface. Because

$$P_{nm} = J_{sc} V_{oc} FF, \quad (2)$$

where J_{sc} is short circuit current density, V_{oc} is the voltage of idling, FF is the fill factor of current-voltage characteristic, then, along with ratio (1), we use the following expression

$$\eta = [J_{sc} V_{oc} FF / (P_r * S_s)] \cdot 100\%. \quad (3)$$

As seen from (3), effectiveness of solar cell increases with an increase in each of the three key output parameters for SC – I_{sc} , V_{oc} and FF.

In turn, the expression for determining V_{oc} takes the following form:

$$V_{oc} = \frac{kT}{q} \ln \left(\frac{J_{sc}}{J_0} + 1 \right), \quad (4)$$

where J_{sc} is the short circuit current density, J_0 is the diode current density of saturation, q is the charge of the electron; k is the Boltzmann constant, T is the temperature of a solar cell.

As shown in (4), the idling voltage depends on J_{sc} and J_0 . Therefore, the high values for V_{oc} require the low values for J_0 .

The current-voltage characteristic fill factor (FF) is determined from ratio:

$$FF = \frac{P_{nm}}{J_{sc} V_{oc}}. \quad (5)$$

In the absence of consistent resistance and the shunting conductivity, the expression for FF can be represented

$$FF = \frac{v_{oc} - \ln(v_{oc} + 0.72)}{v_{oc} + 1}, \quad (6)$$

where

$$v_{oc} = \frac{qV_{oc}}{AkT}. \quad (7)$$

In the presence of consequential resistance (R_s), the expression for the light current-voltage characteristic fill factor (FF) is transformed in the following way

$$FF_s = FF_0 (1 - R_s / R_E), \quad (8)$$

where $R_x = V_{oc} / J_{sc}$ is the characteristic resistance. When sequential resistance (R_s) and the conductivity of the shunt (G) are substantial, the expression for the light current-voltage characteristic fill factor (FF_{s+sh}) takes the form

$$FF_{s+sh} = FF_s \left[1 - \frac{(v_{oc} + 0.72) FF_s}{v_{oc} / (R_E G)} \right]. \quad (9)$$

According to expression (9), it is absolutely obvious that a growth in the value for FF_{s+sh} will be contributed to by a decrease in R_s and G .

Thus, in order to construct a method for restoring the SC efficiency, we must establish a change in the output parameters and the light diode characteristics under the influence of a bias voltage of direct polarity.

5. Results of studying a change in the output parameters and the diode characteristics of ITO/CdS/CdTe/Cu/Au SC

5.1. Studying a change in the output parameters and the light diode characteristics after the accelerated degradation of ITO/CdS/CdTe/Cu/Au SC

The parameters for p-n heterojunctions (HJ) in the examined ITO/CdS/CdTe/Cu/Au SC, which were divided into smooth (S), unidentified (U), and sharp (Sh), depending on the magnitude of a potential barrier and the width of the depletion zone, after 48 months of storage, are given in Table 1. The output parameters and the light diode characteristics, as well as the level of degradation in terms of efficiency following the accelerated degradation, are given in Tables 2, 3.

Table 1

Parameters for n-p heterojunctions of film SC after 48 months of storage

SC	HJ type	Φ_{np} , eV	$W_{np}(0)$, μm	$W_{\text{max}}/W_{\text{min}}$, $\mu\text{m}/\mu\text{m}$	N_{np} , 10^{14} cm^{-3}	a , 10^{18} cm^{-4}
2	S	2.4	3.07	2.85–2.20	–	7.5
6	S	1.0	3.06	3.04–1.90	–	2.8
8	U	0.6	3.07	3.07–1.15	0.5	–
12	U	0.9	3.06	3.06–2.00	0.9	–
16	U	1.4	2.92	2.92–2.24	2.2	–
19	Sh	1.5	3.08	3.08–2.22	1.8	–
20	Sh	1.5	2.93	2.98–2.12	2.0	–

Table 2

Density of photocurrent, diode, and output parameters of SC after accelerated degradation

SC	J_{ph} , mA/cm^2	J_0 , mA/cm^2	A , rel. units	R_s , Ohm cm^2	R_{sh} , Ohm cm^2	J_{sc} , mA/cm^2	V_{oc} , mV	FF , rel. units
2	13.7	$1.6 \cdot 10^{-10}$	1.53	20.5	236	12.6	705	0.46
6	17.2	$9.0 \cdot 10^{-11}$	1.50	10.7	210	16.4	725	0.54
8	6.3	$1.5 \cdot 10^{-12}$	1.34	19.8	893	6.1	758	0.62
12	9.9	$1.7 \cdot 10^{-11}$	1.40	13.6	485	9.7	720	0.60
16	17.1	$1.1 \cdot 10^{-10}$	1.49	12.0	171	16.0	710	0.51
19	15.3	$2.9 \cdot 10^{-10}$	1.66	8.6	316	14.9	749	0.59
20	31.3	$5.5 \cdot 10^{-9}$	1.87	15.9	50	23.6	717	0.35

Table 3

Level of SC degradation in terms of efficiency after 48 months of storage

SC	2	6	8	12	16	19	20
Efficiency coefficient, %	4.1	6.4	2.9	4.2	5.8	6.6	6.0
Degradation, %	54–60	28–38	67–72	53–59	35–44	26–36	33–42

Data given in Table 3 show that the largest degradation was demonstrated by sample No. 8 with an unidentified p-n heterojunction, substantial degradation was exhibited by sample No. 2 with a smooth heterojunction, and No. 12 with an unidentified heterojunction.

5. 2. Studying a change in the output parameters and the diode characteristics of ITO/CdS/CdTe/Cu/Au SC with different types of n-p heterojunctions after exposure to a voltage of direct polarity

The selected samples were exposed to the action of a bias voltage of direct polarity $V_d^{\text{max}} = 675 \pm 5 \text{ mV}$ at maximum duration $\tau_{ex} = 2 \text{ hours}$ under a dark mode at room temperature; next, we acquired the dark VAP.

Fig. 3–8 show the dark current-voltage characteristic for each type of p-n heterojunction, measured before and after the specified exposure, as well as dependences of direct current I_d , that passed through these same SCs at $V_d^{\text{max}} = 0.68 \text{ V}$, on time of the exposure τ_{ex} .

The magnitude of relative change in the output parameters and the diode characteristics for SC with various types of n-p heterojunctions after the shaded SC were exposed to a direct polarity voltage of $V_d^{\text{max}} = 0.68 \text{ V}$ at maximum duration $\tau_{ex} = 2 \text{ hours}$ at room temperature is given in Table 4.

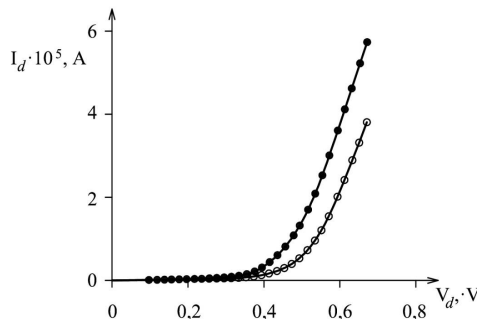


Fig. 3. Static dark volt-ampere characteristics for ITO/CdS/CdTe/Cu/Au SC No. 6: ● – prior to exposure at maximum duration $\tau_{ex} = 2 \text{ hours}$ at $V_n = V_d^{\text{max}}$; ○ – after exposure

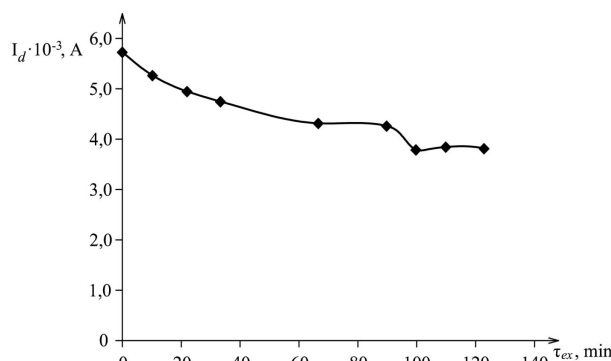


Fig. 4. Dependence of direct current (I_d) passing through these same SCs at $V_d^{\text{max}} = 0,68 \text{ V}$ on the time of exposure τ_{ex} for ITO/CdS/CdTe/Cu/Au SC No. 6

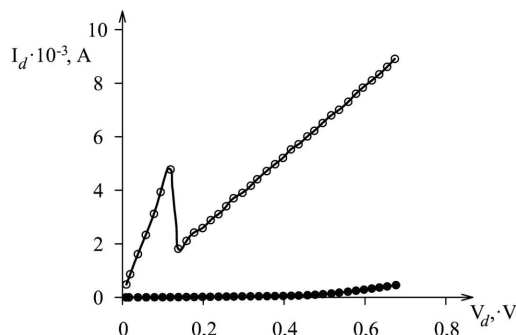


Fig. 5. Static dark volt-ampere characteristics for ITO/CdS/CdTe/Cu/Au SC No. 12: ● – prior to exposure at maximum duration $\tau_{ex} = 2 \text{ hours}$ at $V_d = V_d^{\text{max}}$; ○ – after exposure

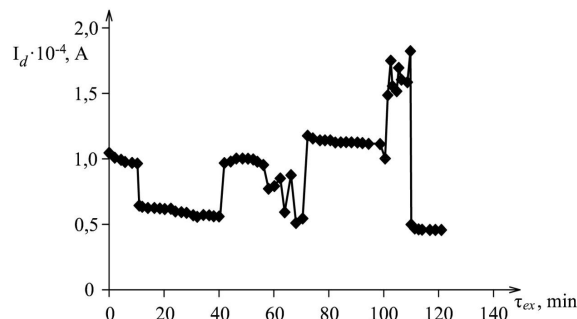


Fig. 6. Dependence of direct current (I_d) passing through these same SCs at $V_d^{\text{max}} = 0,68 \text{ V}$ on the time of exposure τ_{ex} for ITO/CdS/CdTe/Cu/Au SC No. 12

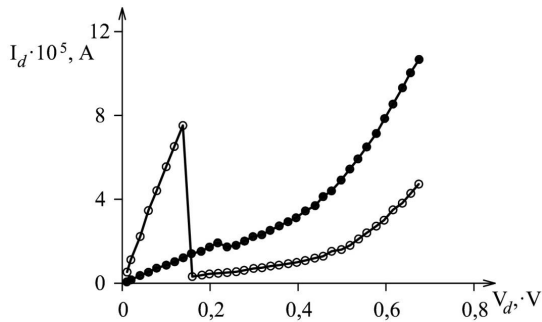


Fig. 7. Static dark volt-ampere characteristics for ITO/CdS/CdTe/Cu/Au SC No. 20: ● – prior to exposure at maximum duration $\tau_{ex}=2$ hours at $V_d = V_d^{max}$; ○ – after exposure

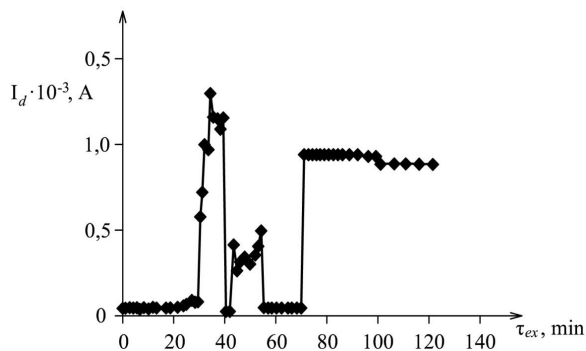


Fig. 8. Dependence of direct current (I_d) passing through these same SCs at $V_d^{max} = 0,68$ V on the time of exposure τ_{ex} for ITO/CdS/CdTe/Cu/Au SC No. 20

5.3. Determining the conditions for restoring the efficiency of film ITO/CdS/CdTe/Cu/Au SC after degradation

Following the exposure over $\tau_{ex}=2$ hours to a voltage of $V_d^{max} = 0,68$ V, the SC operational performance is 62.5 %. An increase in efficiency by 47 % in the examined SC is predetermined mainly by an increase in J_{ph} . For the remaining 43 % of SC within such a category an increase in efficiency is due to an increase in J_{ph} and R_{sh} , as well as due to a decrease in R_s , which led to a rise in FF . And in one of such SCs, along with the indicated changes, an increase in efficiency is also predetermined by a significant decrease in J_0 .

The results described point to a possibility to improve the effectiveness of film SC operation, after degradation, by their further exposure at a moderate temperature under a bias voltage of direct polarity of the n-p heterojunction $V^{max} < V_d^{max} \leq V_{oc}$ for about 2 hours. Such a recovery of efficiency is possible if the diode structure of SC in the process of degradation did not have the time to form the defects in the form of alternating self-restoring electrical micro-breakdowns.

In addition, based on the analysis of results similar to those specified in Fig. 2–7 and Table 4, one can explain the likely mechanisms of influence of the direct polarity voltage on photocurrent, diode, and the output parameters of such SC.

6. Discussion of results of influence of a bias voltage of direct polarity on Fe ITO/CdS/CdTe/Cu/Au SC

When SC is fed voltage $V_d = V_d^{max}$, the forming electric field within a diode structure of SC must enhance the built-in electric field at the rear p-p+ heterojunction and partially inhibit the built-in electric field at the front n-p heterojunction. In this case, at the rear p-p+ heterojunction and in the areas that surrounding it from both sides such processes will be intensified that are associated with the transport of atoms of copper. In addition, there is a restructuring of complexes of point defects, containing copper, and the phase transformations of $Cu_{1,4}Te$ into $Cu_{2-x}Te$. The consequence of these processes should include:

- a certain additional growth in the component of successive resistance from the side of a rear contact;
- a certain reduction in spectral sensitivity over a long wavelength region of solar radiation;
- additional metallization of plots in the joints of longitudinal boundaries of the absorber grains arranged close to the p-p + heterojunction.

However, from the plots of longitudinal joints between the grains of absorber from the side of n-p heterojunction the intra-nodal copper should start moving towards the region of the CdS depletion layer. This process can lead to the dissolution of chains from copper atoms, which formed earlier and partially shunt the heterojunction from the side of CdTe. This circumstance could lead to an increase in shunting resistance. Since the arrival of copper to CdS from the joints of longitudinal boundaries of the absorber grains has a point character, it is possible, in this case, a point formation of additional quantities of the $Cu_{2-s}S$ phase, but this should not significantly affect the magnitude of J_{ph} . Under the influence of the field induced by a bias voltage of direct polarity, particles of Cu_{Cd} from the layer of CdS depletion will start moving to the absorber. Such a move will help reduce the resistance of the CdS layer and can lead to a reduction in the width of the depletion region from the side of absorber. That would en-

Table 4

Change in the output parameters and added characteristics for ITO/CdS/CdTe/Cu/Au SC as a result of action of a bias voltage of direct polarity

SC No./HJ type	Δ Efficiency/Efficiency ₀ , %	$\Delta I_d(\tau_{ex})/I_d(0)$, %	$\Delta J_{ph}/J_{ph}$, %	$\Delta FF/FF$, %	$\Delta J_0/J_0$, %	$\Delta R_s/R_s$, %	$\Delta R_{sh}/R_{sh}$, %
2/S	31.0	-25.0	28.9	5.8	>>-100	-25.0	-86.7
6/S	-4.8	139.8	0.07	-5.2	15.6	13.3	-7.5
8/U	1.7	-27.3	2.2	0.0	-6.9	28.2	151
12/U	-2.3	-55.7*	-6.4	3.5	192	-10.7	7.2
16/U	12.2	-33.3	8.4	3.8	817	-25.7	31.0
19/Sh	2.3	-19.3	2.4	0.0	841	-22.9	-2.6
20/Sh	-81.2	1871	23.8	-52.6	558233	93.7	-82.7

Table 4 shows that four SCs No. 2, No. 8, No. 16, and No. 19, following the exposure to a voltage of direct polarity, demonstrated a partial recovery of efficiency, from 1.7 % for the case of CE No. 8, to 31 % for the case of CE No. 2. The specified increase in the efficiency coefficient occurred after almost a monotonic decline in current strength I_d passing through SC at a constant value. The effectiveness of operation of other SCs following the exposure decreased in relative values from 2.3 % for the case of SC No. 12 to 81.2 % for the case of SC No. 20. That was contributed to by the non-monotonous change in I_d with an increase in τ_{ex} , mainly characteristic of capacitor structures with alternating self-restoring electrical micro-breakdowns.

hance the spectral sensitivity of SC over shortwave and medium-wave regions of solar spectrum. In addition, we do not rule out the dissociation, under the action of the specified field, of the Cu_{2-6}S sublayer, which had formed earlier in the region of n-p heterojunction with the further electrodiffusion of anions of sulfur to the absorber, the transformation of copper cations, formed in Cu_{Cd} and electrodiffusion of Cu_{Cd} following the anions of sulfur. Partial or complete disappearance of the specified sublayer should lead to an increase in J_{ph} . Electrodiffusion of anions of sulfur to the absorber can intensify the sprouting of solid solution of $\text{CdTe}_{1-y}\text{S}_y$ beneath the absorber. The electrodiffusion of additional amount of Cu_{Cd} to the absorber must amplify the described-above and related effects of enhancing the spectral sensitivity of SC. It is obvious that the totality of the examined transformations under the influence of V_d^{max} leads to the increased efficiency of SC operation via an increase in J_{ph} and R_{sh} at a decrease in J_0 and R_s , which is observed experimentally.

It is only natural that in actual SC the ratio of intensities of the progress of the above-examined processes does not always match such a perfect combination of characters in change of J_{ph} , R_{sh} , J_0 and R_s . Probably, for example, in some cases, the flow of copper atoms along the joints at longitudinal boundaries of the absorber grains to the area of n-p heterojunction may outperform the outflow to CdS. In this case it is absolutely clear to us that the powerful emerging shunting should lead to the release of a joule heat within the chain of copper atoms, sufficient to rupture it, which is one of the reasons for self-restoring micro-breakdowns, followed by its resurrection then again a self-restoring micro-breakdown.

Another interesting effect, not described in other papers, is what is observed when reducing V_d to $V_d < 0.2$ V (Fig. 3, 5, 7) – an unintentional switching of SC from the low-conducting state to the high-conducting state. A given effect is well explained by an increase in the reverse action on Cu_i^+ in the region of CdS depletion of the built-in field of n-p heterojunction, which helps saturate the joints of longitudinal boundaries at absorber grains with copper from the side of the specified junction.

Based on the research conducted, we proposed a technique to restore the efficiency of SC after degradation. The technique implies sequential operations related to measuring the dark and light current-voltage characteristic and to the action of a direct polarity voltage. Using the proposed technique, it becomes possible to reject potentially unreliable SC included in solar modules, to prolong the duration and improve the efficiency of operation of potentially reliable devices. This list of successive operations involving SC is as follows. Periodically, at intervals of 24 hours, automatic measurement of light current-voltage characteristic for solar cells that make a solar module with the subsequent analytical treatment for determining the output parameters and the light diode characteristics. When observing a decrease in the output parameters, it is necessary to perform measurements, during dark hours, of the direct branch of the dark current-voltage characteristic at voltages V_d in the range:

$$0 \leq V_d \leq V_d^{\text{act}}, \quad (1)$$

where V_d^{act} is the current value for voltage at which its last-impacting on SC is observed.

In the absence of anomalies in the dependence of current strength I_d on V_d we enter the mode of $V_d = V_d^{\text{act}}$ with the following exposure of SC to voltage over 2 hours and we

simultaneously register the dependence of I_d on the exposure duration τ_{ex} .

For the case of a monotonic descent in the dependence of I_d on τ_{ex} (Fig. 3) the specified operation should be continued for 2 hours, then measure the straight branch of the SC dark current-voltage characteristic when reducing voltage from $V_d = V_d^{\text{act}}$ to zero.

If there is a spontaneous switching of SC from the low-conducting state to the high-conducting state, the efficiency of instruments in the structure can be partially restored, which can be automatically controlled based on the analytical processing of the light current-voltage characteristic at day light.

If the dependence of I_d on τ_{ex} shows the signs of micro-breakdowns or there starts a monotonic ascent of I_d with an increase in τ_{ex} , the recovery via voltage must be stopped; a potentially unreliable SC should be replaced with a new one.

In the absence of anomalies in the dependence of current strength I_d on V_d , we enter the mode of $V_d = V_d^{\text{act}}$ followed by exposing SC to voltage over 2 hours and we simultaneously register the dependence of I_d on the exposure duration τ_{ex} .

For the case of a monotonic descent in the dependence of I_d on τ_{ex} (Fig. 3), the specified operation should be continued for 2 hours, then we measure the straight branch of the SC dark current-voltage characteristic when reducing voltage from $V_d = V_d^{\text{act}}$ to zero.

If there is a spontaneous switching of SC from the low-conducting state to the high-conducting state, the efficiency of instruments in the structure can be partially restored, which can be automatically controlled based on the analytical processing of light current-voltage characteristic at day light.

If the dependence of I_d on τ_{ex} shows the signs of electrical micro-breakdowns or there starts a monotonic ascent of I_d with increasing τ_{ex} , restoring by voltage V_d^{act} must be stopped; a potentially unreliable SC should be replaced with a new one.

6. Conclusions

1. We have experimentally registered the effect of an electrical field of direct polarity on the output parameters and the light diode characteristics of ITO/CdS/CdTe/Cu/Au SC whose efficiency degraded.

2. We have shown a possibility to improve the efficiency of film ITO/CdS/CdTe/Cu/Au SC after degradation by exposing them to a bias voltage of n-p heterojunction if the diode structure of such SC during degradation did not have time to form defects that over a specified time of exposure could lead to the alternating self-restoring electrical micro-breakdowns.

3. We have defined conditions for the restoration of film ITO/CdS/CdTe/Cu/Au SC, based on exposing SC for at least 120 minutes to an electric field whose polarity matches the forward bias of the n-p heterojunction of SC induced by the external constant voltage of magnitude (0.5–0.9) V. Under the influence of an electric field, there occurs the intensification of processes of transporting copper atoms, restructuring of complexes of point defects, containing copper, as well as the phase conversion of $\text{Cu}_{1,4}\text{Te}$. These processes lead to a decrease in the resistance of the CdS layer and to the electrodiffusion to the base layer of sulfur anions and the intra-nodal cations of Cu_{Cd} .

References

1. Nardone M., Albin D. S. Degradation of CdTe Solar Cells: Simulation and Experiment // *IEEE Journal of Photovoltaics*. 2015. Vol. 5, Issue 3. P. 962–967. doi: <https://doi.org/10.1109/jphotov.2015.2405763>
2. Increasing the efficiency of film solar cells based on cadmium telluride / Khrypunov G., Vambol S., Deyneko N., Sychikova Y. // *Eastern-European Journal of Enterprise Technologies*. 2016. Vol. 6, Issue 5 (84). P. 12–18. doi: <https://doi.org/10.15587/1729-4061.2016.85617>
3. Results of studying the Cu/ITO transparent back contacts for solar cells SnO₂:F/CdS/CdTe/Cu/ITO / Deyneko N., Semkiv O., Soshinsky O., Streletc V., Shevchenko R. // *Eastern-European Journal of Enterprise Technologies*. 2018. Vol. 4, Issue 5 (94). P. 29–34. doi: <https://doi.org/10.15587/1729-4061.2018.139867>
4. Deyneko N., Khrypunov G., Semkiv O. Photoelectric Processes in Thin-film Solar Cells Based on CdS/CdTe with Organic Back Contact // *Journal of Nano- and Electronic Physics*. 2018. Vol. 10, Issue 2. P. 02029-1–02029-4. doi: [https://doi.org/10.21272/jnep.10\(2\).02029](https://doi.org/10.21272/jnep.10(2).02029)
5. Degradation of three-junction amorphous Si:H based solar cells / Murashev V. N., Legotin S. A., Krasnov A. A., Dudkin A. A., Zezin D. A. // *Izvestiya Vysshikh Uchebnykh Zavedenii. Materialy Elektronnoi Tekhniki = Materials of Electronics Engineering*. 2013. Issue 4. P. 39–42. doi: <https://doi.org/10.17073/1609-3577-2013-4-39-42>
6. Zezin D. A., Latohin D. V. Ocenka nekotorykh faktorov, vliyayushchih na degradatsiyu solnechnykh elementov na osnove a-Si:H // *Amorfnye i mikrokristallicheskie poluprovodniki: sbornik trudov VIII Mezhdunarodnoy konferencii. Sankt-Peterburg: Izd-vo Politekh. un-ta, 2012. P. 26–27.*
7. Light Induced Defect Creation Kinetics in Thin Film Protocrystalline Silicon Materials and Their Solar Cells / Wronski C. R., Pearce J. M., Koval R. J., Niu X., Ferlauto A. S., Koh J., Collins R. W. // *MRS Proceedings*. 2002. Vol. 715. doi: <https://doi.org/10.1557/proc-715-a13.4>
8. Karpov V. G., Shvydka D., Roussillon Y. Physics of CdTe Photovoltaics: from Front to Back // *MRS Proceedings*. 2005. Vol. 865. doi: <https://doi.org/10.1557/proc-865-f10.1>
9. Cu-related recombination in CdS/CdTe solar cells / Demtsu S. H., Albin D. S., Sites J. R., Metzger W. K., Duda A. // *Thin Solid Films*. 2008. Vol. 516, Issue 8. P. 2251–2254. doi: <https://doi.org/10.1016/j.tsf.2007.08.035>
10. Albin D. S. Accelerated stress testing and diagnostic analysis of degradation in CdTe solar cells // *Reliability of Photovoltaic Cells, Modules, Components, and Systems*. 2008. doi: <https://doi.org/10.1117/12.795360>
11. McMahon T. J., Bernard T. J., Albin D. S. Nonlinear shunt paths in thin-film CdTe solar cells // *Journal of Applied Physics*. 2005. Vol. 97, Issue 5. P. 054503. doi: <https://doi.org/10.1063/1.1856216>
12. Karpov V. G., Shvydka D., Roussillon Y. E2 phase transition: Thin-film breakdown and Schottky-barrier suppression // *Physical Review B*. 2004. Vol. 70, Issue 15. doi: <https://doi.org/10.1103/physrevb.70.155332>
13. Solar photovoltaic electricity: Current status and future prospects / Razykov T. M., Ferekides C. S., Morel D., Stefanakos E., Ullal H. S., Upadhyaya H. M. // *Solar Energy*. 2011. Vol. 85, Issue 8. P. 1580–1608. doi: <https://doi.org/10.1016/j.solener.2010.12.002>
14. Achievements and Challenges of CdS/CdTe Solar Cells / Fang Z., Wang X. C., Wu H. C., Zhao C. Z. // *International Journal of Photoenergy*. 2011. Vol. 2011. P. 1–8. doi: <https://doi.org/10.1155/2011/297350>
15. A study of the CdTe treatment with a Freon gas such as CHF₂Cl / Mazzamuto S., Vaillant L., Bosio A., Romeo N., Armani N., Salviati G. // *Thin Solid Films*. 2008. Vol. 516, Issue 20. P. 7079–7083. doi: <https://doi.org/10.1016/j.tsf.2007.12.124>
16. Thin films of CdIn₂O₄ as transparent conducting oxides / Mamazza R., Balasubramanian U., Morel D. L., Ferekides C. S. // *Proc. of 29th IEEE Photovoltaic Specialists Conference. Anaheim, 2002. P. 616–619.*
17. Highly transparent and conductive ZnO-In₂O₃ thin films prepared by d.c. magnetron sputtering / Minami T., Kakumu T., Takeda Y., Takata S. // *Thin Solid Films*. 1996. Vol. 290-291. P. 1–5. doi: [https://doi.org/10.1016/s0040-6090\(96\)09094-3](https://doi.org/10.1016/s0040-6090(96)09094-3)
18. Pilipenko V. V., Kuprikov V. I., Soznik A. P. Microscopic nucleon-nucleus optical potential with rearrangement effects based on the effective skyrme forces // *International Journal of Modern Physics E*. 2009. Vol. 18, Issue 09. P. 1845–1862. doi: <https://doi.org/10.1142/s0218301309013907>
19. Jeong W.-J., Park G.-C. Electrical and optical properties of ZnO thin film as a function of deposition parameters // *Solar Energy Materials and Solar Cells*. 2001. Vol. 65, Issue 1-4. P. 37–45. doi: [https://doi.org/10.1016/s0927-0248\(00\)00075-1](https://doi.org/10.1016/s0927-0248(00)00075-1)
20. Investigation of the combination of ITO/CdS/CdTe/Cu/Au solar cells in microassembly for electrical supply of field cables / Deyneko N., Semkiv O., Khmyrov I., Khrypynskyy A. // *Eastern-European Journal of Enterprise Technologies*. 2018. Vol. 1, Issue 12 (91). P. 18–23. doi: <https://doi.org/10.15587/1729-4061.2018.124575>
21. Enzenroth R. A., Barth K. L., Sampath W. S. Correlation of stability to varied CdCl₂ treatment and related defects in CdS/CdTe PV devices as measured by thermal admittance spectroscopy // *Journal of Physics and Chemistry of Solids*. 2005. Vol. 66, Issue 11. P. 1883–1886. doi: <https://doi.org/10.1016/j.jpcs.2005.09.022>